Mutant huntingtin fragment selectively suppresses Brn-2 POU domain transcription factor to mediate hypothalamic cell dysfunction

Tomoyuki Yamanaka[1,2], Asako Tosaki[1], Haruko Miyazaki[1], Masaru Kurosawa[1], Yoshiaki Furukawa[1,2], Mizuki Yamada[1] and Nobuyuki Nukina[1,*]

[1]Laboratory for Structural Neuropathology, RIKEN Brain Science Institute, Saitama 351-0198, Japan and [2]Special Postdoctoral Researchers Program, RIKEN, Saitama 351-0198, Japan

In polyglutamine diseases including Huntington's disease (HD), mutant proteins containing expanded poly-glutamine stretches form nuclear aggregates in neurons. Although analysis of their disease models suggested a significance of transcriptional dysregulation in these diseases, how it mediates the specific neuronal cell dysfunction remains obscure. Here we performed a comprehensive analysis of altered DNA binding of multiple transcription factors using R6/2 HD model mice brains that express an N-terminal fragment of mutant huntingtin (mutant Nhtt). We found a reduction of DNA binding of Brn-2, a POU domain transcription factor involved in differentiation and function of hypothalamic neurosecretory neurons. We provide evidence supporting that Brn-2 loses its function through two pathways, its sequestration by mutant Nhtt and its reduced transcription, leading to reduced expression of hypothalamic neuropeptides. In contrast to Brn-2, its functionally related protein, Brn-1, was not sequestered by mutant Nhtt but was upregulated in R6/2 brain, except in hypothalamus. Our data indicate that functional suppression of Brn-2 together with a region-specific lack of compensation by Brn-1 mediates hypothalamic cell dysfunction by mutant Nhtt.

INTRODUCTION

Polyglutamine diseases including Huntington's disease (HD) are autosomal-dominant, adult-onset neurodegenerative disorders caused by expansion of CAG repeats in certain causative genes (1–3). In HD, mutant huntingtin containing expanded polyglutamine forms nuclear aggregates in neurons. Studies using HD model mice have identified many genes whose expression is altered by mutant huntingtin (4–7). Mutant huntingtin has also been reported to interact and/or sequester several transcription factors including CREB-binding protein (CBP) (8,9), TBP (10–12), SP1 (13,14), TAFII130 (13), p53 (9) and NF-Y (15). These observations suggest an importance of transcriptional dysregulation in HD and other polyglutamine diseases (16,17), although how it mediates neuronal cell dysfunction remains obscure.

In this study, we screened affected transcription factors using a new strategy in which alterations in their DNA binding were comprehensively analyzed in brains of a commonly used HD mouse model (R6/2) which expresses an N-terminal (exon1) fragment of mutant huntingtin (mutant Nhtt). We found the reduction of DNA binding of Brn-2, a POU domain transcription factor involved in differentiation and function of hypothalamic neurosecretory neurons. The reduction of functional Brn-2 was also observed in isolated hypothalamus of R6/2. Furthermore, in addition to reduced mRNA expression of vasopressin (VP) and oxytocin (OT) as previously reported (6), reduced expression of corticotropin releasing horman (CRH) mRNA was observed without obvious cell loss. Interestingly, suppression of Brn-2 function by mutant Nhtt was caused by its sequestration and its reduced transcription in hypothalamus. In contrast, Brn-1, another POU domain factor functionally related to Brn-2, was not sequestered by mutant Nhtt but was upregulated in R6/2 brains, except in hypothalamus, suggesting region-specific lack of compensation by Brn-1 in hypothalamus. These data

---

*To whom correspondence should be addressed. Tel: +81 484679702; Fax: +81 484624796; Email: nukina@brain.riken.jp
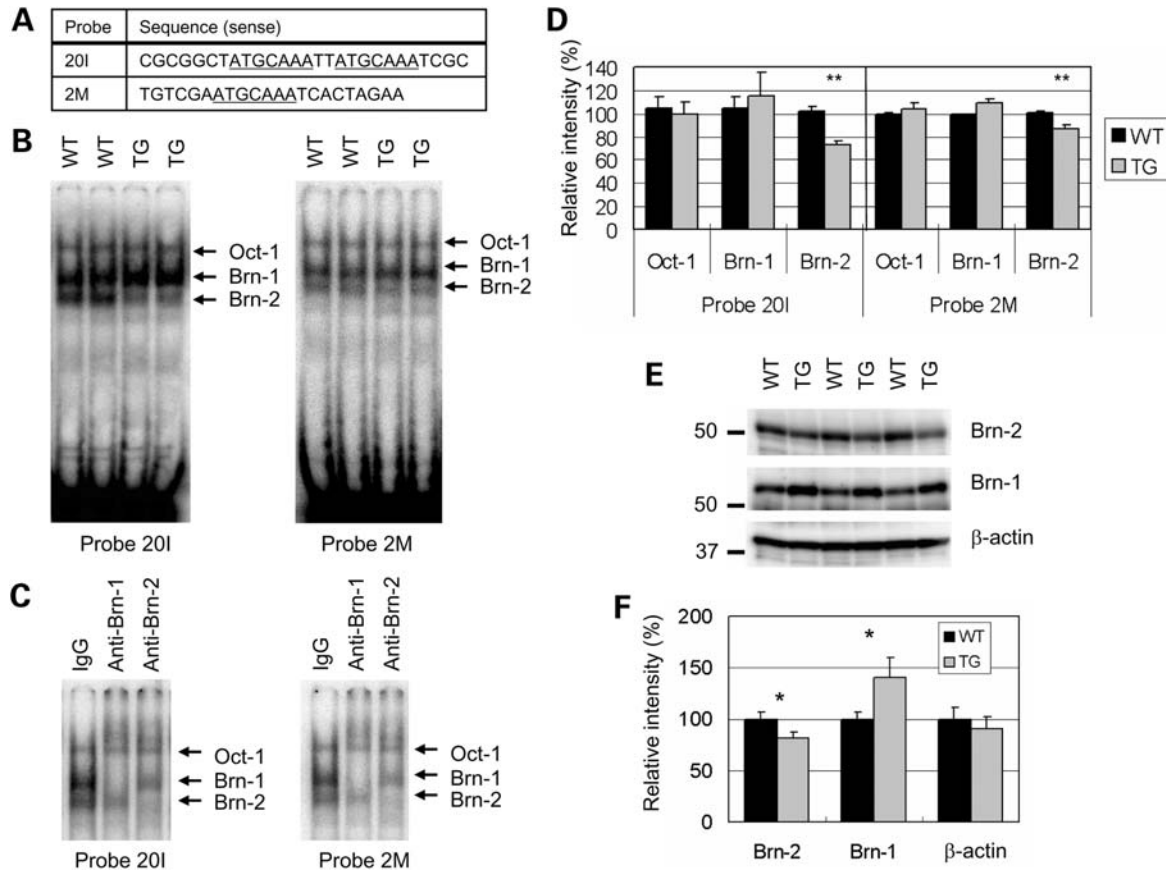
Figure 1. Reduced DNA binding of Brn-2 in R6/2 mouse brain cortex. (**A**–**D**) Cortical lysates prepared using high-salt buffer from 12-week-old R6/2 (TG; $n = 3$) or control (WT; $n = 3$) mice were subjected to EMSA using probe 20I (left) or 2M (right). (A) Nucleotide sequences of sense oligonucleotides of the probes. The binding consensuses of POU domain factors are underlined. (B) Three shifted bands corresponding to the probe-complex containing Oct-1, Brn-1 and Brn-2 are indicated. (C) Super-shift assay using anti-Brn-1, anti-Brn-2 or IgG for probe 20I (left) or 2M (right). (D) Quantification of the amount of protein complexes with probe 20I (left) and 2M (right). Values are means ± SD (**$P < 0.01$). (**E**) The cortical lysates of R6/2 or control mice were subjected to western blot analysis using antibodies against Brn-2 (C-2AP), Brn-1 (C-2AP) and β-actin. (**F**) Quantification of the amount of Brn-2, Brn-1 and β-actin. Values are means ± SD (*$P < 0.05$).

indicate that functional suppression of Brn-2 together with a hypothalamus-specific lack of Brn-1 upregulation leads to hypothalamic cell dysfunction in R6/2 brain. Our finding provides a novel mechanism underlying specific neuronal cell dysfunction induced by mutant huntingtin.

RESULTS

Identification of Brn-2 as a novel mutant Nhtt-affected factor through functional screening using R6/2 mouse brain cortex lysates

Our previous observation that a reduction of DNA binding of NF-Y in cortical lysates of R6/2 HD model mice (15) led us to try to identify novel mutant Nhtt-affected transcription factors by monitoring alterations of their DNA binding in the lysates. For this purpose, we used Protein DNA array technology (Panomics), which allowed us to measure DNA binding activities of multiple transcription factors using a 345-probe set containing different binding sequences for transcription factors. Through the screening, some of the probes showed altered protein-binding in R6/2 samples (data not shown). We then

performed an electrophoretic mobility shift assay (EMSA) by using the probes labeled with ^{32}P, and finally nine probes were confirmed to show the alterations of the amounts of protein-DNA complexes in R6/2 cortical lysates. Among them, probes 1F and 1K contain binding sites for known affected factors, NF-Y and EGR1, respectively (Supplementary Material, Fig. S1) (4,15). As for EGR1, its probe binding and its reduced mRNA expression in R6/2 were confirmed by super-shift assay and RT–PCR analysis, respectively (Supplementary Material, Fig. S1). These data support that our screening system worked well.

Interestingly, two other probes, 20I (NF-A3) and 2M (OCT), contain ATGCAAA sequences, which is the binding site for POU domain transcription factors (Fig. 1A) (18). Using these probes, we observed three shifted bands by EMSA (Fig. 1B). The upper, middle and lower bands correspond to the probe complex containing Oct-1 (Pou2f1), Brn-1 (Pou3f3) and Brn-2 (Pou3f2, N-Oct-3), respectively (19). Indeed, the middle and lower bands were further shifted by the addition of antibodies specific to Brn-1 and Brn-2, respectively (Fig. 1C, Supplementary Material, Fig. S2A). Importantly, the Brn-2-probe complex was specifi-
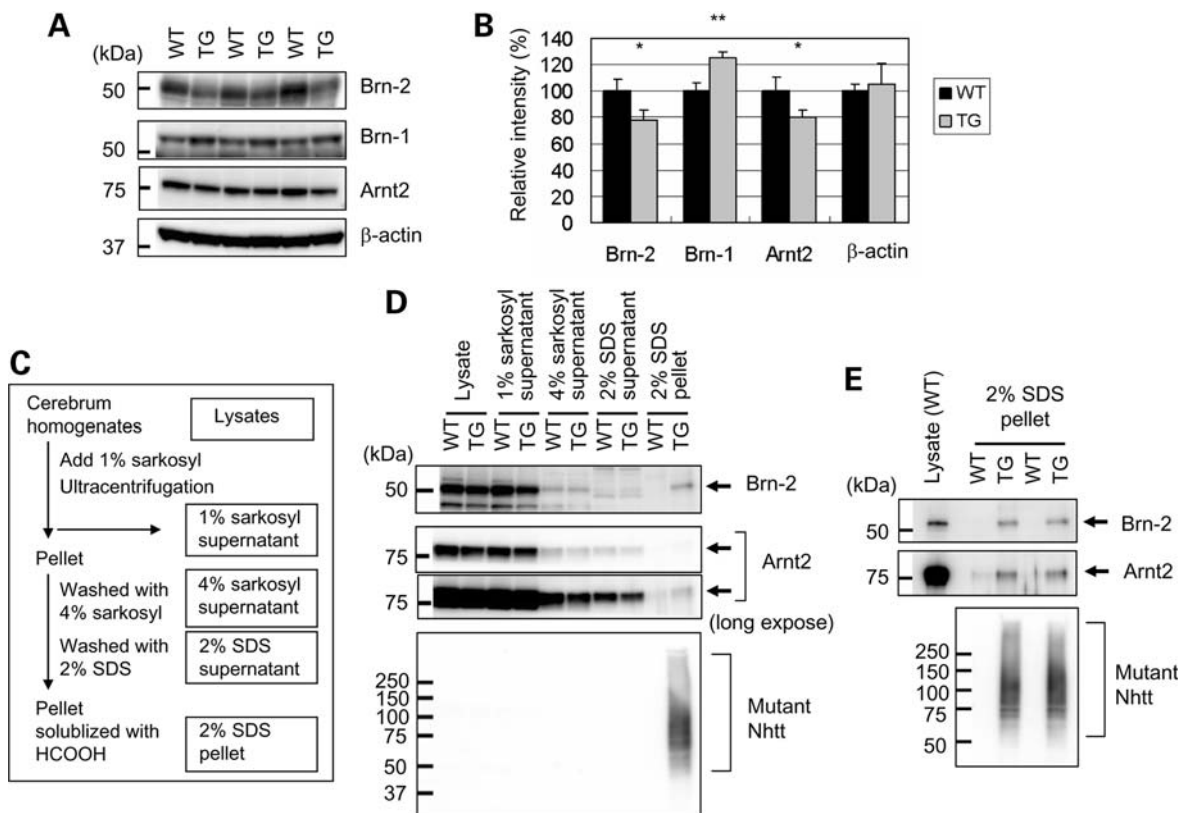
Figure 2. Reduction of Brn-2 and Arnt2 proteins and their co-fractionation with mutant Nhtt into SDS-insoluble fraction in R6/2 cerebrum. (**A**) Cerebral lysates prepared using SDS sample buffer from 12-week-old R6/2 (TG; $n = 3$) or control mice (WT; $n = 3$) were subjected to western blot analysis using antibodies against Brn-2 (C-2AP), Brn-1 (C-2AP), Arnt2 and β-actin. (**B**) Quantification of the amount of Brn-2, Brn-1, Arnt2 and β-actin. Values are means $\pm$ SD (*$P <$ 0.05, **$P <$ 0.01). (**C** and **D**) Cerebrum homogenates (Lysates) of 12-week-old R6/2 (TG) or control (WT) mice were fractionated as shown in (C), and each fraction was subjected to SDS–PAGE and western blot analysis using antibodies against Brn-2 (C-2AP), Arnt2 and polyglutamine (1C2) (D). (**E**) 2% SDS pellet fractions prepared from other R6/2 (TG) or control mice (WT) were subjected to western blot analysis using antibodies against Brn-2 (C-2AP), Arnt2 or polyglutamine (1C2).

cally reduced in R6/2 samples, whereas probe complexes containing Oct-1 and Brn-1 were not affected (Fig. 1B). Quantified data showed that the binding of Brn-2 was reduced by 10–20% of control levels in R6/2 cortical lysates (Fig. 1D). The difference in degree of the reduction between these probes may be due to the difference in the number of binding sites (Fig. 1A). These data indicate that Brn-2 is specifically affected by mutant Nhtt among the POU domain factors active in the cortical lysates.

Western blot analysis revealed the reduction of Brn-2 protein in the R6/2 cortical lysates used for Protein DNA array and EMSA (Fig. 1E and F). Reduced immunoreactivity of Brn-2 in R6/2 cortex was also observed by immunostaining with anti-Brn-2 (Supplementary Material, Fig. S3). These data suggest that reduction of DNA binding of Brn-2 is caused by reduction of its protein level in the R6/2 cortex lysates.

Brn-2 was sequestered by mutant Nhtt in R6/2 brain

Western blot analysis of cerebrum lysates prepared using SDS sample buffer also revealed reduction of Brn-2 protein in R6/2 (Fig. 2A and B), whereas the mRNA expression of Brn-2 was not affected in R6/2 cerebrum (Supplemental Fig. S4A). These data suggest that protein reduction of Brn-2 is not caused by

its reduced transcription. We then examined whether Brn-2 was sequestered by mutant Nhtt by fractionating homogenate (lysates) of WT and R6/2 cerebrum as indicated in Figure 2C. As previously reported (20), smear bands for mutant Nhtt were detected by anti-polyglutamine antibody in a 2% SDS pellets of R6/2 but not WT (Fig. 2D and E), suggesting the formation of SDS-insoluble aggregate of mutant Nhtt in R6/2 cerebrum. Importantly, Brn-2 was also observed in the 2% SDS pellet fraction of R6/2 but not WT in addition to its reduction in 1% sarkosyl supernatant fraction of R6/2 (Fig. 2D and E), suggesting that Brn-2 forms an SDS-insoluble complex with mutant Nhtt in R6/2 cerebrum. On the contrary, Brn-1 was not observed in the 2% pellet fraction (data not shown), supporting the specific sequestration of Brn-2 by mutant Nhtt. Taken together, these observations indicate that mutant Nhtt specifically sequesters Brn-2 by rendering it insoluble, leading to reduction of functional Brn-2 in R6/2 brain.

Mutant Nhtt selectively forms SDS-insoluble complex with Brn-2 in transfected neuro2a cells

How is Brn-2 specifically sequestered by mutant Nhtt? In contrast to the high conservation at C-terminal DNA-binding POU
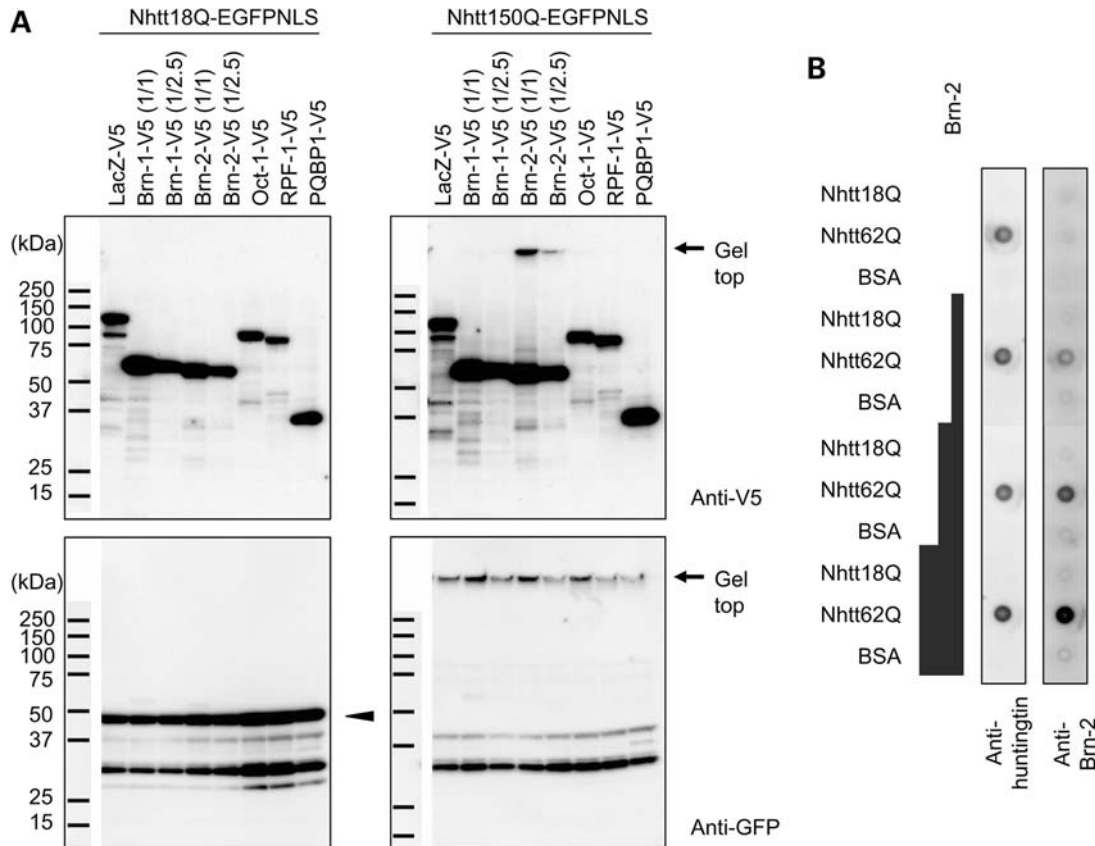
Figure 3. Brn-2 forms SDS-insoluble complex with mutant Nhtt in neuro2a cells and *in vitro*. (**A**) Co-aggregation of Brn-2 with mutant Nhtt in transfected neuro2a cells. Neuro2a cells were transfected with expression vector for Brn-1, Brn-2, Oct-1, RPF-1, PQBP-1 or LacZ tagged with V5 together with expression vector for Nhtt18Q-EGFP-NLS (left) or Nhtt150Q-EGFP-NLS (right). After 24 h, cells were subjected to SDS–PAGE and western blot analysis using anti-V5 (upper) or anti-GFP (lower) antibody. Bands for Nhtt18Q-EGFP-NLS are indicated by arrowhead and positions at the top of the gel are indicated by arrows. Bands for soluble Nhtt150Q-EGFP-NLS were not observed in the gel, possibly due to its efficient insolubilization, but they were detected at the top of the gel. In the case of Brn-1 and Brn-2, 1/2.5 the amount of plasmid DNA was used to make their expression levels similar to those of other proteins. (**B**) Co-aggregation of Brn-2 with mutant Nhtt *in vitro*. HRV-3C-treated Nhtt18Q, Nhtt62Q or BSA (0.2 mg/ml) was co-incubated with different concentrations of HRV-3C-treated His-TF-Brn-2 (0, 0.2, 0.5 or 1 mg/ml) at 37°C as indicated to the left of panels. After 20 h, the samples were subjected to filter trap assay and the aggregated proteins were detected with anti-huntingtin or anti-Brn-2 (C-2AP).

domains, N-terminal regions are very diverse among Brn-2, Brn-1 and Oct-1 (Supplementary Material, Fig. S5). Interestingly, only Brn-2 contains a polyglutamine stretch (23Q) at its N-terminal region. In addition, Brn-2 has been shown to localize to the mutant huntingtin inclusion in transfected cells (21). We checked interactions of Oct-1, Brn-1 or Brn-2 with mutant Nhtt aggregates by using transfected neuro2a cells co-expressing Oct-1, Brn-1 or Brn-2 tagged with V5 together with Nhtt containing a pathological stretch of glutamine (150Q) fused with EGFP and SV40 NLS (Nhtt150Q-EGFP-NLS). As shown in Figure 3A, Nhtt150Q-EGFP-NLS formed SDS-insoluble aggregates, which were detected at the top of the gel by anti-GFP antibody. These bands were not observed when Nhtt containing a normal stretch of polyglutamine (Nhtt18Q-EGFP-NLS) was used (Fig. 3A). Anti-V5 staining showed top bands for Brn-2-V5 in the cells expressing Nhtt150Q-EGFP-NLS, but not in the cells expressing Nhtt18Q-EGFP-NLS, whereas top bands for Oct-1-V5 and Brn-1-V5 were not observed in these cells (Fig. 3A). We also analyzed another POU domain factor, RPF-1, because it has a polyglutamine stretch (19Q) at the

N-terminal region (Supplementary Material, Fig. S5); however, a top band was not observed on the gel (Fig. 3A). This suggests that in addition to the polyglutamine stretch, its surrounding sequence may be important for the formation of SDS-insoluble aggregates with mutant Nhtt in neuro2a cells. We also examined PQBP-1 because it was first identified as a Brn-2 binding protein and its interaction with soluble polyglutamine or mutant Ataxin-1, a causative protein for spinocerebellar ataxia 1, have been reported (22,23). However, incorporation of PQBP-1-V5 into Nhtt150Q-EGFP-NLS aggregates was not observed (Fig. 3A), suggesting that Brn-2 binding to mutant Nhtt aggregates is not through PQBP-1.

Immunofluorescence analysis of transfected neuro2a cells showed the preferential localization of Brn-2-V5 to Nhtt150Q-EGFP-NLS inclusions compared with Oct-1-V5 and Brn-1-V5 (Supplementary Material, Fig. S6A). Quantitative analysis revealed that most cells showed disappearance of diffuse Brn-2-V5 in association with its accumulation in Nhtt150Q-EGFP-NLS inclusions (Supplementary Material, Fig. S6B). The effective sequestration of Brn-2-V5 with
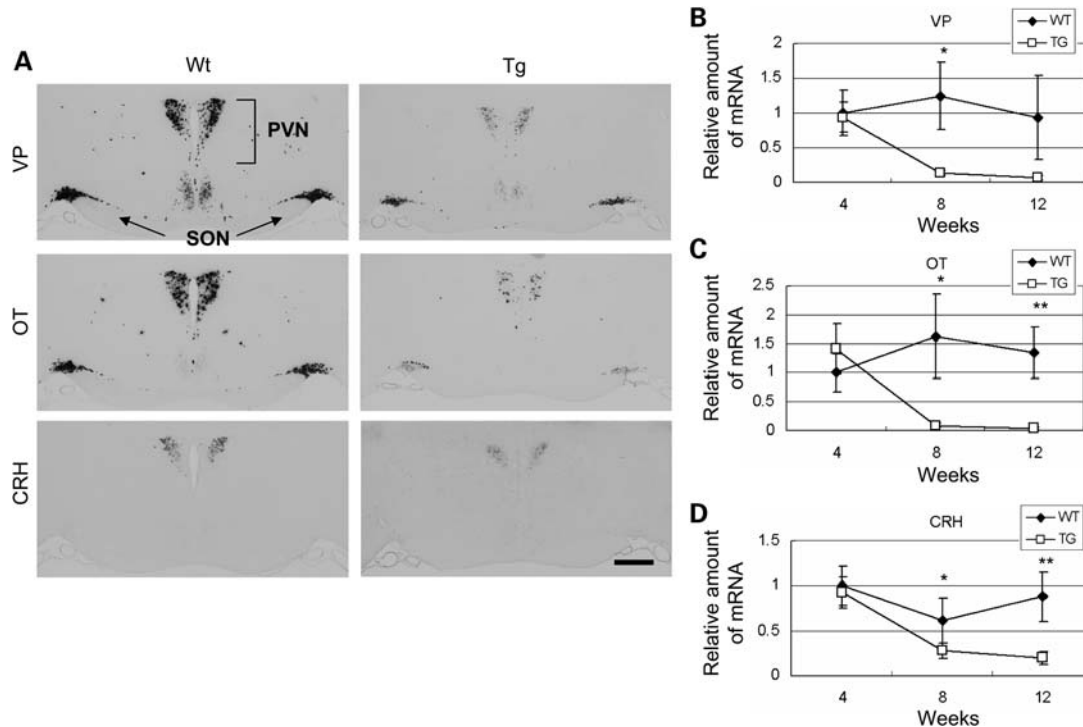
Figure 4. Reduced mRNA expressions of OT, VP and CRH in R6/2 brain hypothalamus. (**A**) *In situ* hybridization of coronal sections from 12-week-old R6/2 (TG) or control (WT) mouse brain using antisense probe for VP, OT or CRH. PVN and SON regions are indicated. Scale bar = 400 μm. (**B–D**) Quantitative RT–PCR analysis of VP (B), OT (C) or CRH (D) in cerebrum of 4-, 8- or 12-week-old R6/2 (TG; $n = 4$) or control (WT; $n = 4$) mice. Values are means ± SD (*$P < 0.05$, **$P < 0.01$).

Nhtt150Q-EGFP-NLS was further confirmed by cell fractionation analysis, that is, distinct population of Brn-2-V5 was detected with Nhtt150Q-EGFP-NLS but not Nhtt18Q-EGFP-NLS in high-salt buffer-insoluble fraction in association with reduction of soluble Brn-2-V5 (Supplementary Material, Fig. S7A–C). In contrast, LacZ-V5 stayed soluble in the cells expressing either Nhtt18Q/150Q-EGFP-NLS (Supplementary Material, Fig. S7A–C). Taken together, these data indicate that among these POU domain factors, only Brn-2 is efficiently sequestered by mutant Nhtt in neuro2a cells.

We also examined the interaction of Brn-2 with soluble Nhtt using transfected neuro2a cells by immunoprecipitation assay according to the procedure used for analysis of interactions between soluble huntingtin and TFIIF subunits (24). However, coprecipitation of Brn-2 with soluble Nhtt18Q/62Q proteins was not observed (data not shown), suggesting that Brn-2 preferentially interacts with the aggregated form of mutant Nhtt in these cells.

Brn-2 directly incorporated into mutant Nhtt aggregates *in vitro*

To test whether Brn-2 directly interacts with mutant Nhtt *in vitro*, Brn-2 cDNA was cloned into pCold TF vector; thereby Brn-2 was expressed as a fusion protein with a His tag and a trigger factor (TF) under a cold shock promoter in *E. coli*, after which His-TF-Brn-2 protein was then purified by nickel column (Supplementary Material, Fig. S8A and C). GST-Nhtt containing 18Q or 62Q was also purified from *E. coli* (Supplementary Material, Fig. S8B and C). After removal of a GST tag with HRV-3C protease, Nhtt18Q/62Q was incubated at 37°C for 20 h. As shown in Figure 3B, Nhtt62Q but not 18Q, formed SDS-insoluble aggregates that were detected by filter trap assay. Importantly, when His-TF-Brn-2 treated with HRV-3C was co-incubated with Nhtt18Q/62Q, Brn-2 also formed SDS-insoluble aggregates with Nhtt62Q but not Nhtt18Q in a concentration-dependent manner (Fig. 3B). On the contrary, Brn-2 did not form SDS-insoluble aggregates if BSA was used as a control (Fig. 3B), indicating that Brn-2 itself could not form the aggregates and requires mutant Nhtt for its aggregation. Taken together, these data revealed that Brn-2 was directly incorporated into mutant Nhtt aggregates *in vitro*.

Increase in Brn-1 protein in R6/2 brain

Because increased levels and activity of Brn-1 have been observed in Brn-2 knockout mouse brain (19,25), we checked the Brn-1 protein level in R6/2 brain lysates. Western blot analysis revealed increases in Brn-1 in cerebrum and cortical lysates of R6/2 (Figs 1E and F and 2A and B). Furthermore, increased immunoreactivity of Brn-1 was observed in R6/2 cortex by anti-Brn-1 staining (Supplementary Material, Fig. S3). Because no increase in Brn-1 mRNA expression in R6/2 brain cerebrum was observed by RT–PCR (Supplementary Material, Fig. S4B), upregulation of Brn-1 protein was not caused by its increased transcription but by other mechanisms such as protein stabilization or
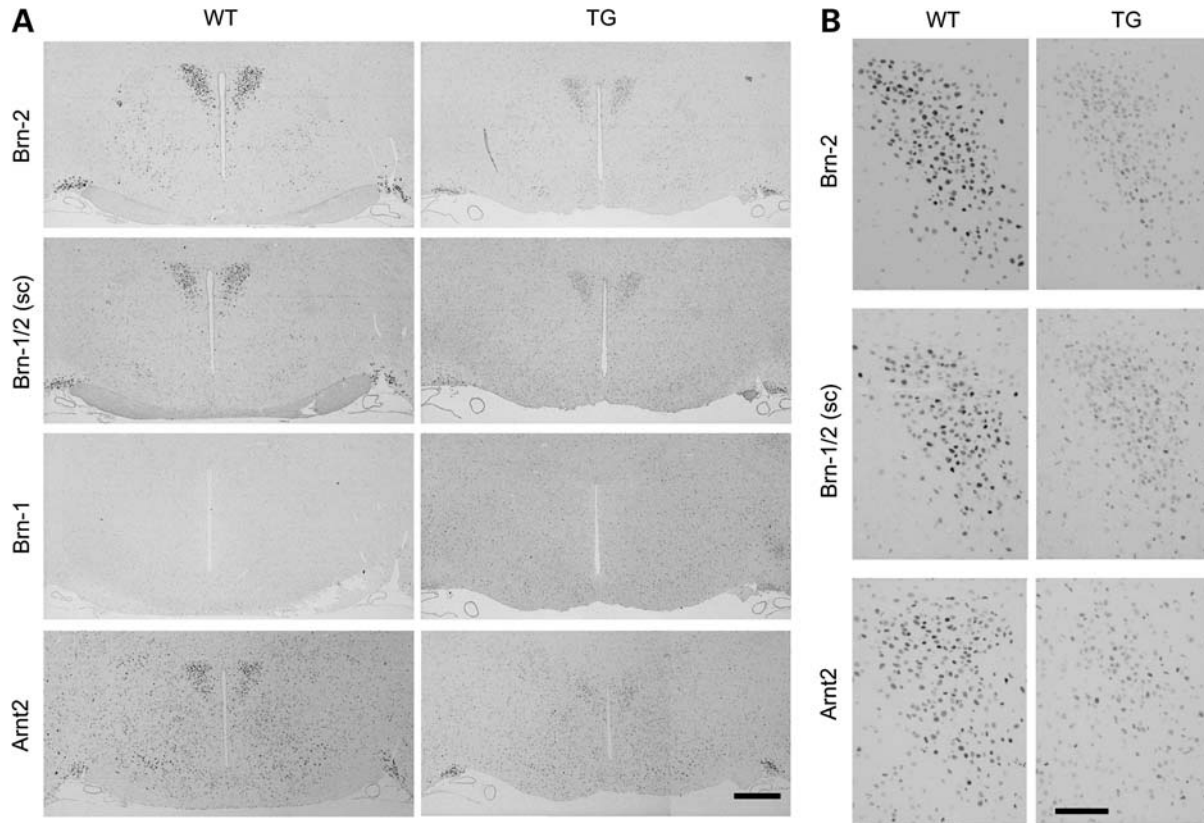
Figure 5. Reduction of Brn-2 and Arnt2 proteins in R6/2 hypothalamus. (**A**) Coronal sections prepared from paraffin-embedded brain of 12-week-old R6/2 (TG) or control (WT) mice were stained with antibody against Brn-2 (C-2AP), Brn-1/2 (sc), Brn-1 (C-2AP) or Arnt2. (**B**) Magnified images of the PVN stained with antibody against Brn-2 (C-2AP), Brn-1/2 (sc) or Arnt2. Scale bars = 400 μm (A) and 100 μm (B).

increased translation. Although the mechanism is unclear, these data support the reduced function of Brn-2 in R6/2 brain, and further suggest that the induction of Brn-1 protein in R6/2 brain may be a compensation mechanism for the reduced function of Brn-2.

Reduction of VP, OT and CRH in R6/2 brain hypothalamus

Studies using Brn-2 homozygous knockout mice revealed the importance of Brn-2 for the development of two hypothalamic neurosecretory neurons, magnocellular and parvocellular neurons (18,19,25). The magnocellular neurons in paraventricular nucleus (PVN) and sporaoptic nucleus (SON) produce VP) and OT, whereas parvocellular neurons in PVN produce CRH (Fig. 4A). Although Brn-2 homozygous knockout leads to complete loss of these neurons (19,25), Brn-2 heterozygous knockout results in reduced expression of mRNAs for VP and OT to less than half of normal levels without any morphological alteration in the hypothalamus (19), indicating that Brn-2 is also important for expression of these hypothalamic neuropeptides.

In situ hybridization analysis of R6/2 revealed a distinct reduction of mRNAs of OT and VP in PVN and SON of hypothalamus, as we previously reported (Fig. 4A) (6). In addition, clear reduction of CRH mRNA was also observed in PVN

(Fig. 4A). These were further confirmed by RT–PCR analysis using cerebrum (Fig. 4B–D). Reduced protein expressions of VP and OT were also observed by immunohystochemical analysis as reported previously (Supplementary Material, Fig. S9A) (26). Furthermore, reduction of CRH protein has been reported (27). It should be noted that hematoxylin staining revealed no distinct alteration in hypothalamic PVN in R6/2 (Supplementary Material, Fig. S9B), suggesting no severe cell loss in these regions of R6/2. These results indicate that transcription of VP, OT and CRH is reduced in the hypothalamus of R6/2 similar to Brn-2 heterozygous knockout mice, which showed the reduction of those neuropeptide expressions.

The magnocellular neurons expressing VP and OT project their axons directly into the posterior lobe of the pituitary gland. Because loss of posterior lobe has been shown in Brn-2 homozygous mice (19,25), we examined the morphology of the pituitary gland in R6/2 mice. Although the posterior lobe of R6/2 was slightly smaller than that of wild-type (Supplementary Material, Fig. S10A), the reduction was not as severe as it is in Brn-2 homozygous mice. In addition, lower but distinct OT and VP signals were observed in the posterior lobe of R6/2 mouse (Supplementary Material, Fig. S10B; data not shown). These data also support the idea that the reduced expression of neuropeptides in R6/2 is not caused by neuronal cell loss in the hypothalamus.
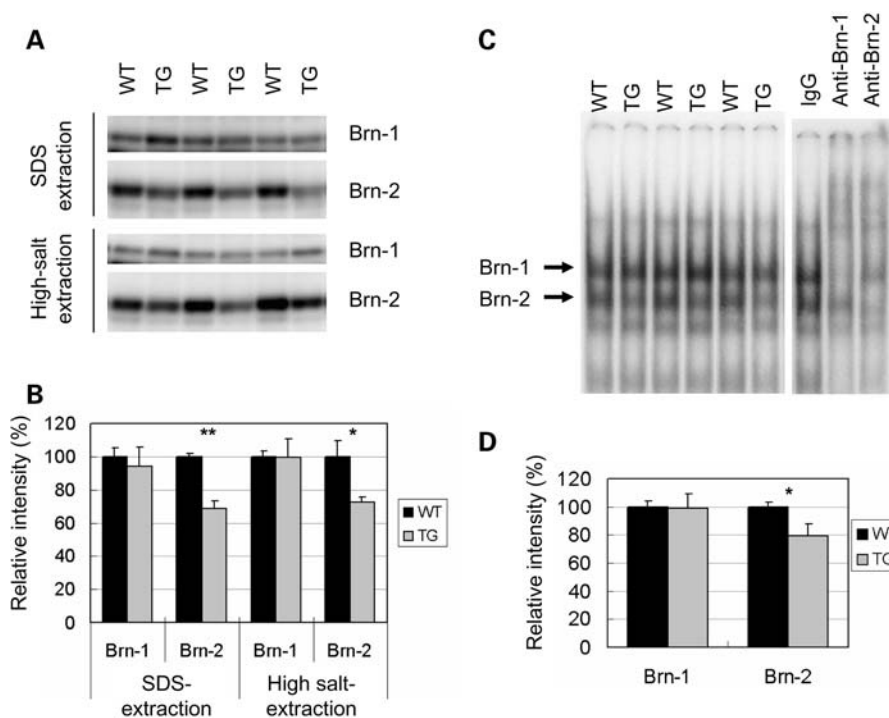
Figure 6. Reduction of DNA binding of Brn-2 in isolated hypothalamus of R6/2 mice. (**A**) Isolated hypothalamus from 12-week-old R6/2 (TG; $n = 5$) or control (WT; $n = 5$) mice were lysed with SDS sample buffer (upper panels) or high-salt buffer (lower panels), and were subjected to western blot analysis using anti-bodies against Brn-2 (C-2AP) or Brn-1 (C-2AP). (**B**) Quantification of the amount of Brn-2 and Brn-1. (**C**) The lysates prepared using high-salt buffer were subjected to EMSA using probe 20I (left). Super-shift assay using antibodies against Brn-2 (C-2AP) or Brn-1 (C-2AP) (right). (**D**) Quantification of the amount of protein-probe complexes. Values are means $\pm$ SEM ($*P < 0.05$, $**P < 0.01$).

Reduction of protein levels and DNA binding of Brn-2 in R6/2 hypothalamus

We next examined whether Brn-2 protein was also reduced in R6/2 hypothalamus. In control mice, anti-Brn-2 signals were predominantly observed in PVN and SON neurons in its hypothalamus (Fig. 5A), consistently with previous observations (19,25). Importantly, these signals were clearly reduced in 12-week-old R6/2 hypothalamus (Fig. 5A). Similar results were also observed by staining with another antibody, anti-Brn-1/2 (Fig. 5A), which recognizes both Brn-2 and Brn-1 (Supplementary Material, Fig. S2A and B). In contrast, specific staining was not observed by anti-Brn-1 in PVN and SON in wild-type mice as previously reported (Fig. 5A) (25), suggesting that anti-Brn-1/2 stained only Brn-2 in these regions. Magnified images showed that although the level of Brn-2 was severely reduced, the number of Brn-2-positive cells seemed to stay consistent (Fig. 5B), suggesting that the reduction of Brn-2 is not caused by a loss of Brn-2-positive cells. Accumulations of Nhtt and ubiquitin, as well as for-mations of inclusions positive for them were confirmed in PVN cells of R6/2 mouse (Supplementary Material, Fig. S11). Thus, Brn-2 protein was reduced in association with accumulation of mutant Nhtt inclusions in 12-week-old R6/2 hypothalamus.

Because RT–PCR analysis revealed that the mRNAs of VP, OT and CRH was not reduced at 4 weeks but started to decrease at 8 weeks after birth in R6/2 mouse brain (Fig. 4B–D), we used immunohistochemistry to examine the

Brn-2 protein level in mice of these ages. We found that Brn-2 together with VP and OT were reduced in hypothalamus of 8-week-old R6/2 mouse but not that of 4-week-old R6/2 mouse (Supplementary Material, Fig. S12A and B). Thus, the reduction of Brn-2 protein was correlated with the reductions of hypothalamic neuropeptides in R6/2 hypothala-mus.

The reduction of Brn-2 protein in hypothalamus of 8- and 12-week-old R6/2 mice was confirmed by western blot analysis for isolated hypothalamus lyzed with SDS sample buffer (Fig. 6A and B and Supplementary Material, Fig. S12C and D). In contrast, Brn-1 protein levels were not significantly changed (Fig. 6A and B and Supplementary Material, Fig. S12C and D). Importantly, EMSA using lysates prepared by high-salt buffer revealed a specific reduction in DNA binding of Brn-2 in 12-week-old R6/2 hypothalamus (Fig. 6C and D), in addition to its reduced protein level (Fig. 6A and B). Thus, functional Brn-2 was specifically reduced, together with its reduced protein level in R6/2 hypothalamus.

Reduction of Brn-2 mRNA in R6/2 hypothalamus

Unexpectedly, *in situ* hybridization analysis showed reduction of Brn-2 mRNA in PVN and SON (Fig. 7A). This was con-firmed by RT–PCR analysis using isolated hypothalamus; that is, in addition to reductions of VP and OT, Brn-2 mRNA was also reduced in R6/2 hypothalamus (Fig. 7D). Almost no VP or OT mRNAs were detected in the remaining
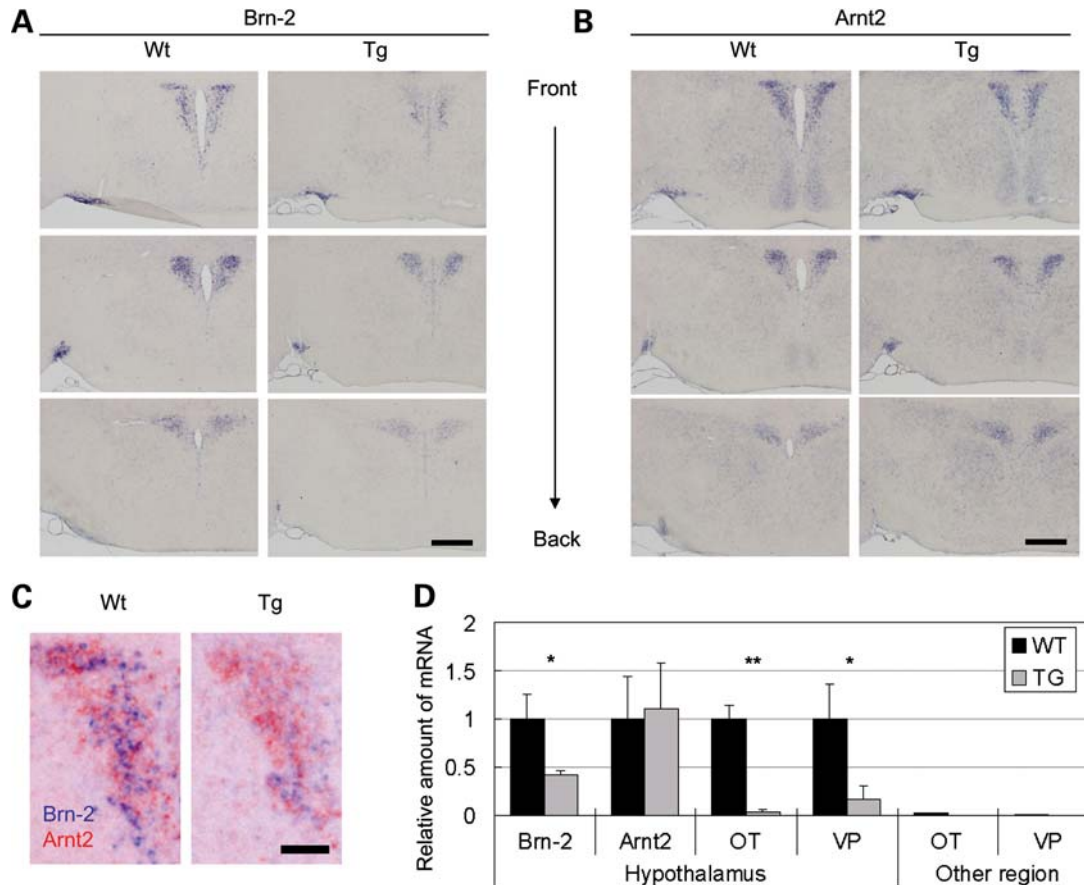
Figure 7. Reduction of mRNA expression of Brn-2 but not Arnt2 in R6/2 hypothalamus. (**A** and **B**) Coronal sections from 12-week-old R6/2 (TG) or control (WT) mouse brain were subjected to *in situ* hybridization using antisense probe for Brn-2 (A) or Arnt2 (B). Three sections from front to back with 200 μm intervals were shown. (**C**) Brn-2 and Arnt2 signals in PVN were artificially labeled with blue and red, respectively, and merged. Note the drastic reduction of blue signals (Brn-2) compared with red signals (Arnt2) in R6/2 mouse. (**D**) Quantitative RT–PCR analysis of Brn-2, Arnt2, VP and OT of isolated hypothalamus from 12-week-old R6/2 (TG; $n = 3$) or control mice (WT; $n = 3$). As for VP and OT, RT–PCR data for other cerebral regions of one WT and one TG after removal of the hypothalamus are also shown. Values are means $\pm$ SD (*$P < 0.05$, **$P < 0.01$). Scale bars = 400 μm (A and B) and 100 μm (C).

cerebrum after removal of the hypothalamus, supporting the idea that the hypothalamic PVN and SON are contained in isolated tissues (Fig. 7D). The reduction of Brn-2 mRNA seems to be specific to hypothalamus because no alteration of Brn-2 mRNA was observed if we used cerebrum for RT–PCR as described earlier. In addition, *in situ* hybridization analysis showed no distinct reduction of Brn-2 mRNA in R6/2 cortex (data not shown). Thus, in hypothalamus, reduced transcription of Brn-2 may also contribute to the reduction of functional Brn-2 in R6/2 mice.

Reduction of Arnt2 protein and its sequestration by mutant Nhtt in R6/2 brain

Arnt2, one of the basic helix-loop-helix Per-Arnt-Sim (bHLH-PAS) family proteins, is another important transcription factor for differentiation of neurons in PVN and SON (28–30). Importantly, Arnt2 and its co-factor, Single-minded 1 (Sim1), are required for expression of Brn-2 during hypothalamic development (28–31). Thus, we next examined the possibility of altered expression of Arnt2 in R6/2 hypothalamus.

We first checked the expression of Arnt2 mRNA in hypothalamus. *In situ* hybridization analysis revealed no clear reduction of Arnt2 mRNA in PVN and SON of R6/2 hypothalamus (Fig. 7B). Because sequential sections were used for the detection of Brn-2 and Arnt2, we compared their mRNA expressions by artificially labeling their signals. Merged pictures show a drastic reduction of Brn-2 signals (blue) compared with Arnt2 signal (red) in R6/2 PVN (Fig. 7C). RT–PCR analysis using isolated hypothalamus further supports no distinct reduction of Arnt2 mRNA in R6/2 mice hypothalamus (Fig. 7D).

In contrast to the mRNA expression analysis, immunohistochemical analysis using anti-Arnt2 antibody revealed distinct reduction of Arnt2 signals in hypothalamic PVN of R6/2 mice (Fig. 5A and B). The reduction was also observed in cortical regions of R6/2 mice (Supplementary Material, Fig. S3). Furthermore, western blot analysis showed a reduction of Arnt2 protein in R6/2 cerebrum (Fig. 2A and B). Because no alteration of Arnt2 mRNA was also observed in R6/2 cerebrum by RT–PCR analysis (Supplementary Material, Fig. S4C), these data indicate that reduction of Arnt2 protein is not caused by its reduced transcription.

Because Arnt2 contains a glutamine-rich region at the C-terminal end, one possibility to explain the reduction of Arnt2 protein is its sequestration by mutant Nhtt. Indeed, Arnt2 protein was detected in an SDS-insoluble pellet prepared from R6/2, but not WT, cerebrum (Fig. 2D and E). In addition, western blot analysis using transfected neuro2a cells showed the SDS-insolubilization of part of Anrt2-V5 in the cells expressing Nhtt150Q-EGFP (Fig. 8A). This was confirmed by filter trap assay, although the amount of trapped Arnt2-V5 was less than that of Brn-2-V5 (Fig. 8B). Furthermore, partial accumulation of Artn2-V5 to the Nhtt150Q-EGFP inclusion was also observed by immunofluorescent microscopy (Supplementary Material, Fig. S6A and B). It should be noted that similar to Brn-2, Arnt2 did not coprecipitate with soluble Nhtt18Q/62Q proteins from transfected neuro2a cells (data not shown), suggesting the preferential interaction of Arnt2 with the aggregated form of mutant Nhtt in these cells. These data suggest that Arnt2 also co-aggregates with and is sequestered by mutant Nhtt, which leads to reduction of soluble Arnt2 in R6/2 brain.

DISCUSSION

In this study, we performed screening of affected transcription factors in R6/2 HD model mouse brains using a new strategy and identified a novel factor, Brn-2, whose DNA binding was reduced in these brains. Importantly, Brn-2 was sequestered by mutant Nhtt by co-aggregation. We also found evidence that mutant Nhtt reduced Brn-2 transcription in hypothalamic neurons possibly through sequestering Brn-2-upstream regulator, Arnt2. Finally, we showed the reduction of functional Brn-2 in addition to reduced expressions of VP, OT and CRH in hypothalamus of R6/2 without obvious cell loss. These data indicate that Brn-2 loses its function through two pathways, its sequestration by mutant Nhtt and its reduced transcription, resulting in the reduced transcriptions of VP, OT and CRH (Fig. 9). Thus, our screening-based analysis could identify novel mutant Nhtt target, Brn-2, which mediates hypothalamic cell dysfunction in HD model mouse brain.

Identification of novel affected transcription factors by mutant Nhtt *in vivo*

Although previous studies have identified potential targets of mutant huntingtin, such as CBP, TBP, SP1, TAFII130 and p53 (32,33), several *in vivo* studies did not fully support their sequestrations and/or suppressions but rather suggested upregulations of some of these in HD model mouse brain (15,34–37). Thus, their direct roles for transcriptional dysregulation in HD are still controversial.

Recently, we have performed screening of interacting proteins of mutant Nhtt aggregates purified from cultured neuro2a cells and identified NF-Y transcription factor as a novel protein sequestered by mutant Nhtt (15). Importantly, sequestration/suppression of NF-Y leads to reduced HSP70 expression in HD model mouse brain. Thus, our previous study supported an importance of screening-based approach for analysis of the transcriptional dysregulation induced by mutant huntingtin. However, with the exception of CA150, a
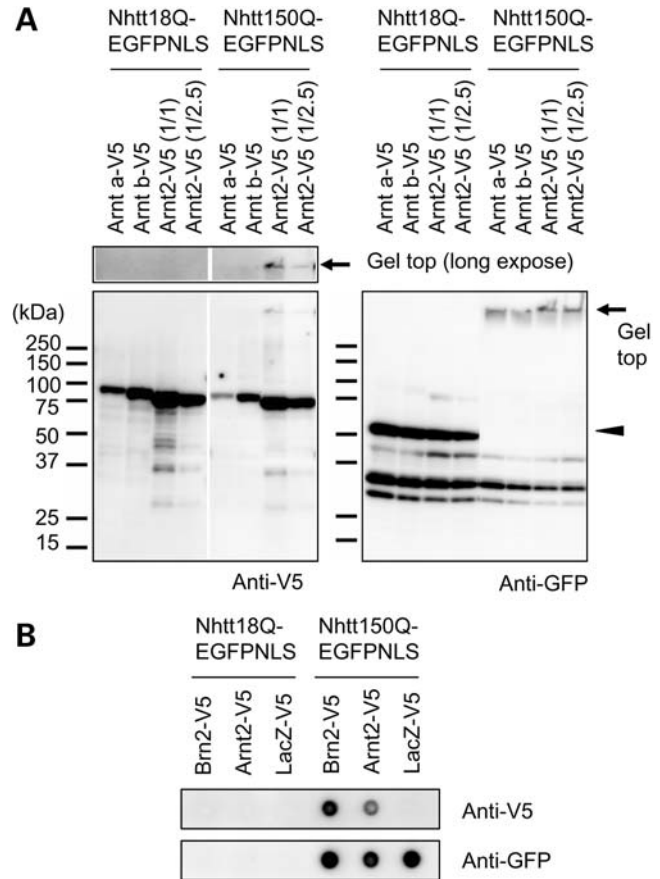

Figure 8. Arnt2 forms SDS-insoluble aggregates with mutant Nhtt in neuro2a cells. (**A**) Neuro2a cells were transfected with expression vector for Arnt (isoform a or b) or Arnt2 tagged with V5 together with expression vector for Nhtt18Q-EGFP-NLS or Nhtt150Q-EGFP-NLS. After 24 h, cells were subjected to SDS–PAGE and western blot analysis using antibody against V5 (left) or GFP (right). Bands for Nhtt18Q-EGFP-NLS are indicated by arrowhead and positions at the top of the gel are indicated by arrows. Bands for soluble Nhtt150Q-EGFP-NLS were not observed in the gel but detected at the top of the gel. In the case of Arnt2, 1/2.5 the amount of plasmid DNA was used to make its expression levels similar to those of other proteins. (**B**) Neuro2a cells were transfected with expression vector for Brn-2, Arnt2 or LacZ tagged with V5 together with expression vector for Nhtt18Q-EGFP-NLS or Nhtt150Q-EGFP-NLS. After 24 h, cells were lysed with SDS-sample buffer and were subjected to filter trap assay. The aggregated proteins were detected with anti-V5 or anti-GFP.

known huntingtin aggregate-interacting protein (38), no other transcription factors were obtained through this system possibly because of limitation of use of the cultured cell line as a brain neuronal model (see what follows).

This problem was overcome in this study by using HD model mouse brain as a material and by performing the screening using new strategy in which alterations in DNA binding of transcription factors were comprehensively analyzed by Protein DNA array. We identified Brn-2 as a novel protein affected by mutant Nhtt, in addition to known affected factors, NF-Y and EGR1. In addition, detailed analysis further identified Arnt2 as another protein sequestered by mutant Nhtt in the model mouse brain. Our study is sharp contrast to the previous studies identifying the targets described above because they were found on the basis of their interactions
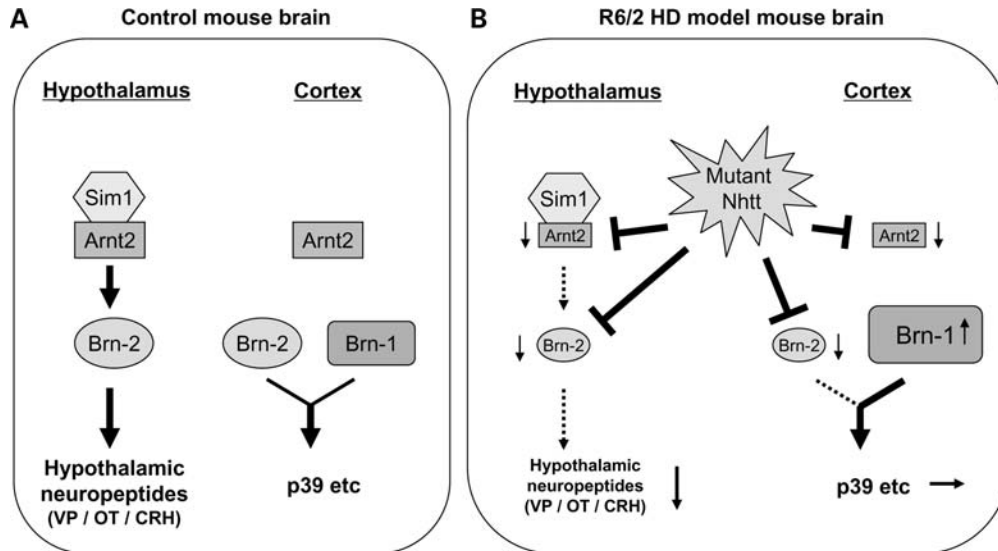
Figure 9. Hypothetical model. (**A**) In control mouse brain, Brn-2 is involved in the expression of neuropeptides in hypothalamus, whereas both Brn-2 and Brn-1 are involved in the expression of their target genes including p39 in cortex. Arnt2 regulates Brn-2 expression only in hypothalamus by forming a protein complex with its hypothalamus-specific co-factor, Sim1. (**B**) In R6/2 HD model mouse brain, mutant Nhtt sequesters Brn-2, leading to a reduction of functional Brn-2. Mutant Nhtt also sequesters Arnt2 to reduce the functional Arnt2-Sim1 complex, which further contributes to the reduction of functional Brn-2 by its reduced transcription. The suppression of Brn-2 as well as a lack of upregulation of Brn-1 leads to reduced expressions of neuropeptides in hypothalamus. In contrast, expressions of cortical Brn-1/2 targets including p39 are not affected possibly because of compensation of Brn-2 suppression by upregulated Brn-1.

with mutant huntingtin. Importantly, expressions of Brn-2 and Arnt2 are not observed in neuro2a cells (T.Y., N.N., unpublished data), supporting the significance of use of *in vivo* system for analysis of the transcriptional dysregulation induced by mutant huntingtin.

Involvement of differential transcriptional dysregulation by mutant Nhtt in its tissue/cell-specific effects on R6/2 mice

We found the induction of Brn-1 protein expression in cortical region of R6/2 HD model mice. Importantly, increase in Brn-1 DNA binding has been shown in Brn-2 knockout mice brain (19). In addition, increased cortical staining of Brn-1 has been observed in a Brn-2 knockout mouse, although the authors did not explicitly report this phenomenon (25). Thus, these observations also support the reduction of functional Brn-2 in R6/2 mouse brain. Importantly, the induction of Brn-1 expression was not observed in hypothalamic PVN and SON, where only Brn-2 is expressed, suggesting that co-expression of these two proteins is required for Brn-1 upregulation upon Brn-2 dysfunction.

Brn-1 and Brn-2 double-knockout mice show suppressed cortical development, due to reduced transcription of several important regulators including p39, a CDK5 regulatory subunit, during embryogenesis (39,40). It should be noted that our *in situ* hybridization analysis revealed no reduction in cortical p39 expression in 12-week-old R6/2 mouse brain (Supplementary Material, Fig. S13). In addition, RT–PCR analysis showed no distinct reduction of p39 in 12-week-old R6/2 mouse cerebrum (data not shown). These data suggest that total Brn-1/2 activity is not affected in R6/2 brain. Although we could not directly observe the lack of compensatory

effect by Brn-1 in hypothalamus by *in situ* hybridization analysis because there is no p39 expression in this region of control mice (Supplementary Material, Fig. S13), our data strongly support the idea that region-specific upregulation of Brn-1 compensates for Brn-2 dysfunction in the cortex but not in the hypothalamus of R6/2 mice, resulting in hypothalamic cell dysfunction in these mice (Fig. 9).

Our data also suggest that the reduction of Brn-2 mRNA is specific to hypothalamus in R6/2 mice, whereas the protein level of its upstream regulator, Arnt2, was decreased in whole cerebrum including hypothalamus and cortex in these mice. One possible mechanism could be the limited expression of Sim1, an Arnt2 functional co-factor. This would confine the Anrt2 dysfunction-induced suppression of Brn-2 expression to the hypothalamus of R6/2 because Arnt2 homozygous mutation has been reported to lead to suppression of Brn-2 expression only where Arnt2 co-localizes with Sim1 during hypothalamic development (30). Consistently, *in situ* hybridization analysis revealed that Sim1 mRNA signals were exclusively observed in hypothalamus but not in other regions, including cortex, in both 12-week-old control and R6/2 mouse brains (data not shown). Thus, Arnt2 could be functional for Brn-2 expression only when it forms a protein complex with Sim1 in hypothalamus, and Arnt2 sequestration by mutant Nhtt may lead to reduction of the functional Arnt2–Sim1 complex, resulting in hypothalamus-specific reduction of Brn-2 expression in R6/2 brain (Fig. 9).

Interestingly, increased expression and/or transcriptional activity in HD model mouse brain has been observed for other transcription factors reported to be affected by mutant huntingtin. These include increased mRNA expression of NF-Y components (15), increased protein/mRNA expression of SP1 (36), increased protein and transcriptional activity of

p53 (37) and increase in CREB activity and its mediated CRE transcription (35). It should be noted that p53 has been shown to be induced in a cell-type-specific manner; that is, mutant huntingtin induces p53 expression to suppress HSP70 induction in cortical neurons, which are highly sensitive to mutant huntingtin-induced degeneration, but not in cerebellar granule cells, which are insensitive to it (41). Thus, precise analysis focused on increased expression/activity of these proteins might lead to identification of a novel mechanism underlying the region- and cell-type-specific degeneration observed in HD.

Dysregulated expression of hypothalamic neuropeptides in HD model mice and HD patients

Although the expression of CRH was shown to be reduced in R6/2 mice, CRH downstream factors, pituitary adrenocorticotropic hormone (ACTH) and serum corticosterone have been shown to be increased in R6/2 mice (42). This seems to be caused by an alternative compensatory mechanism because expressions of ACTH and corticosterone have been shown to be not affected in Brn-2 homozygous knockout mice despite the loss of hypothalamic neurons expressing CRH in those mice (25). Importantly, increase in ACTH and corticosterone has been also reported in HD patients (42,43), which may contribute some of HD clinical symptoms, such as impaired glucose metabolism and muscular wasting (44).

Recently, Wood *et al.* (26) reported increased thirst and drinking in R6/2, which may be related to reduction of VP in its hypothalamus. Increased thirst was also observed in HD patients (clinical stage III), although serum VP was increased in these patients. One possibility is that hypothalamic neurons in HD patients up to this stage could increase VP release to maintain body water balance, as the authors suggested. Because R6/2 mice express a very long glutamine stretch (more than 120Q), VP could be decreased in advanced clinical HD or juvenile HD. Expression of a shorter fragment of huntingtin in R6/2 mice may also enhance and/or spread the mutant huntingtin's effects. Interestingly, recent studies using human and animal models have revealed an importance of VP and OT for social cognition/behavior (45). Further studies will be necessary to clarify the pathological significance of altered transcriptions of VP, OT and CRH observed in the HD model mice.

In addition to VP, OT and CRH, we have previously found reduced transcription of other hypothalamic neuropeptides including neuropeptide Y, prepro-thyroid-stimulating hormone (TSH)-releasing hormone and prepro-somatostatin. Furthermore, recent studies have found several degenerations in some hypothalamic neurons of HD patients and HD model mice (44); that is, loss of somatostatin-containing neurons in the lateral tuberal nucleus in HD patients (46), and loss of orexin-containing neurons in the lateral hypothalamic area of HD model mice and HD patients (47). It should be noted that the reductions of VP and OT are also observed in brains of model mice for another polyglutamine disease, dentatorubral-pallidoluysian atrophy (DRPLA) (48). Further studies will be needed to deepen our understanding of molecular mechanisms and pathological significances of dysfunction/ degeneration of several hypothalamic neurons induced by mutant huntingtin or other polyglutamine disease proteins.

Conclusion

In summary, our screening-based approach identified novel affected factors by mutant Nhtt, which mediate the region-specific cellular dysfunction in HD model mice. Further studies focused on selective and differential transcriptional alterations may identify a novel mechanism underlying the cell/tissue-specific dysfunction observed in HD and other polyglutamine diseases.

MATERIALS AND METHODS

Mice

The mouse experiments were approved by the animal experiment committee of the RIKEN Brain Science Institute. Mice were maintained and bred in accordance with RIKEN guidelines. Heterozygous htt exon 1 transgenic male mice of the R6/2 strain were obtained from Jackson Laboratory (Bar Harbor, ME, USA). In this paper, only males of R6/2 (over 120 CAG repeats) and age-matched control mice were used for experiments. For most of the histological analysis including hematoxylin staining, immunohistochemistry and *in situ* hybridization, we used R6/2 and control littermates. For biochemical analysis including Protein DNA array, EMSA, brain fractionation and RT–PCR, we used several littermates to obtain enough R6/2 and control samples.

Antibodies

Polyclonal antibodies, Brn-2 (C-2AP) and Brn-1 (C-2AP), were generated against the C-terminal 14 amino acid of mouse Brn-2 or Brn-1, respectively. Each antibody was purified by respective antigen peptide conjugated to SulfoLink Coupling Gel (PIERCE Biotechnology, Rockford, IL, USA). Anti-htt (EM48; MAB5374), anti-polyglutamine (1C2; MAB1574), anti-VP (AB1565), anti-OT (AB911) and anti-ubiquitin (MAB1510) were from Chemicon International (Temecula, CA, USA); anti-Brn-2 (sc-6029; referred to as anti-Brn-1/2 (sc) in this paper because it recognizes both Brn-1 and Brn-2), anti-EGR1 (sc-110) and anti-Arnt2 (sc-5581) were from Santa Cruz Biotechnology Inc.; anti-V5 (R960-25) was from Invitrogen; anti-β-actin (A5441) was from Sigma-Aldrich.

Expression vectors

The mouse cDNAs for Brn-1, Brn-2 and Oct-1 were cloned from mouse brain cDNA by standard PCR methods. The mouse cDNAs for Arnt (isoforms a and b), Arnt2, RPF-1 and PQBP-1 were kindly provided as FANTOM3 clones (49). These cDNAs were subcloned into a pcDNA3.1/ V5-His or pcDNA-DEST40 vector (Invitrogen) for expression in mammalian cells. pcDNA3.1-LacZ/V5-His was from Invitrogen. cDNAs for N terminal huntingtin (exon 1) containing a polyglutamine stretch (18Q, 62Q or 150Q) fused with EGFP and SV40 NLS subcloned into pcDNA3.1 vector (Invitrogen) were described previously (50). cDNA for Brn-2 was subcloned into pCold TF (Takara) for expression in *E. coli.*

Brain lysis, Protein DNA array and EMSA

Isolated tissues (cortex or hypothalamus) from mouse brains were homogenized for 10 strokes with lysis buffer containing 20 mM Hepes, pH 7.9, 25% glycerol, 150 mM NaCl, 1.5 mM MgCl$_2$ and complete protease inhibitor using a glass homogenizer, after which time NaCl was added to a final concentration of 420 mM. After incubation on ice for 20 min, the lysates were centrifuged at 800g for 5 min, and further clarified by centrifugation at 20 000g for 30 min. The supernatants were used for Protein DNA array and EMSA. Protein DNA array (Panomics) was performed according to the manufacturer's protocol. The array we used here was Combo Array, which contains 345 spots for probes. Briefly, the tissue lysates were pre-incubated with a mixture of biotin-labeled probes containing binding sequences for different transcriptional factors to allow the formation of protein/probe complexes. After separation of the complex from the free probes by column filtration, the probes in the complexes were extracted and hybridized to the array. Then, hybridized probes were labeled with streptavidin-HRP and detected by Chemiluminescent regent. EMSA was performed as described previously (15).

Cell culture, transfection and fractionation

Neuro2a cells were maintained in DMEM supplemented with 10% FBS and penicillin-streptomycin in an atmosphere containing 5% CO$_2$. Transfection was performed by Lipofectamine 2000 (Invitrogen) according to the manufacturer's protocol. For fractionation, frozen cells were suspended with 200 µl of lysis buffer containing 20 mM Hepes, pH 7.9, 25% glycerol, 150 mM NaCl, 1.5 mM MgCl$_2$ and complete protease inhibitor, after which NaCl was added to a final concentration of 420 mM. After incubation on ice for 20 min, the lysates were subjected to ultracentrifugation (TLA55; Beckman Coulter) at 50 000 rpm for 30 min at 4°C, and a supernatant was saved as a lysis buffer-soluble fraction. The pellet was washed once with the lysis buffer, and incubated in 100 µl of formic acid at 37°C for 1 h. After being dried up using a Speed-Vac, 200 µl of lysis buffer was added to the pellet. The supernatant and pellet fractions were redissolved/sonicated and boiled in SDS sample buffer and subjected to western blot analysis as described previously (51). Chemiluminescent signals were obtained and quantified using LAS-1000 (Fuji film).

Immunofluorescence microscopy and immunohistochemistry

Transfected neuro2a cells were fixed with 4% paraformaldehyde/PBS and stained as described previously (15). Paraffin-embedded brain coronal sections (5 µm thick) were deparaffinized, autoclaved in 10 mM citrate buffer (pH 6.0) at 120°C for 5 min and stained as described previously (52).

Brain fractionation

Homogenization and fractionation of 12-week-old R6/2 or control mice cerebrum shown in Fig. 2C were performed as described previously (20). The lysates or fractions were boiled in SDS sample buffer and subjected to western blot analysis as described previously (51). Chemiluminescent signals were obtained and quantified using LAS-1000 (Fuji film).

RNA preparation, cDNA synthesis and quantitative real time PCR

Preparations of total RNA, reverse transcription and cDNAs synthesis from mouse cerebrum were performed as described previously (52). Primers and TaqMan probes for quantitative real-time PCR were designed based on Primer Express software (Applied Biosystems). Nucleotide sequences are listed in Supplementary Material, Table SI. The real-time PCR was performed by TaqMan (VP, OT, Brn-2) or SYBR green (GAPDH, CRH, Brn-1, Arnt2, EGR1) according to the manufacturer's protocol (Applied Biosystems). All values obtained were normalized with respect to levels of GAPDH mRNA.

In situ hybridization

Mouse cDNAs for CRH (1–564 bp; full cording sequence), Brn-2 (800–1335 bp in coding sequence), Arnt2 (1600–2136 bp in coding sequence) and p39 (529–1110 bp in coding sequence) were subcloned into pGEM-T-easy vector, and used as a template for *in vitro* transcription of digoxigenin-labeled riboprobes. We also used IMAGE clones 640127 and 16180045, containing mouse cDNAs for OT and VP, respectively, for probe synthesis as described previously (6). The probes were subjected to *in situ* hybridization using 20 µm brain sections of mice fixed with 4% paraformaldehyde/PBS by perfusion as described previously (6).

Protein purification from *E. coli*

GST-Nhtt containing polyglutamine stretches of 18Q or 62Q were purified from transformed *E. coli* (BL21) carrying pGEX-6P-Nhtt 18Q or 62Q, respectively, as described previously (50). For purification of His-TF-Brn-2, we incubated transformed *E. coli* (BL21) carrying pCold-TF-Brn-2 grown in LB medium with 0.1 mM isopropyl-beta-D-thiogalactopyranoside (IPTG) at 16°C for overnights. The cells were suspended with PBS containing complete protease inhibitor. After addition of Triton-X 100 (final conc.; 1%) and lysozyme (final conc.; 0.5 mg/ml), cells were sonicated and subjected to centrifugation at 12 000 rpm for 30 min. The supernatants were incubated with HIS-Select Nickel Affinity Gel (SIGMA) at 4°C for 2 h. After washing the gel with buffer A (50 mM Tris–HCl, pH 8.0,150 mM NaCl, 0.035% β-mercaptoethanol, 10% glycerol) and 10 mM imidazole/buffer A, the protein was eluted with 200 mM imidazole/buffer A. The eluted proteins were dialyzed with buffer A for 2 h at 4°C using a Slide-A-Lyzer Cassette (PIERCE).

Filter trap assay

0.2 mg/ml of GST-Nhtt proteins or BSA in 25 µl of buffer A was incubated with ~1 µl of HRV-3C protease (Novagen) at 4°C for 2 h to cut off Nhtt from GST. Different amounts of

His-TF-Brn-2 (0, 0.2, 0.5 or 1 mg/ml) in 25 µl of buffer A were also incubated with ∼1 µl of HRV-3C protease at 4°C for 2 h to cut off Brn-2 from His-TF. These proteins were mixed and incubated at 37°C for 20 h. After boiling in SDS sample buffer, the samples were filtered by cellulose acetate membrane with 0.2 µm pore size (ADVANTEC), and washed with buffer containing 2% SDS, 50 mM Tris−HCl, pH8.0, 10% glycerol. After blocking the membrane with 5% skim milk in TBST, trapped proteins were detected by incubation with anti-huntingtin (EM48) or anti-Brn-2 (C-2AP), followed by HRP-conjugated anti-mouse or rabbit IgG, respectively.

Statistical analysis

All data were first analyzed by F-test. For $P > 0.05$, the data were analyzed by Student's t-test; otherwise data were analyzed by Welch's t-test. $P < 0.05$ by t-test was considered statistically significant.

SUPPLEMENTARY MATERIAL

Supplementary Material is available at *HMG* online.

REFERENCES

1. Walker, F.O. (2007) Huntington's disease. *Lancet*, **369**, 218–228.
2. Landles, C. and Bates, G.P. (2004) Huntingtin and the molecular pathogenesis of Huntington's disease. Fourth in molecular medicine review series. *EMBO Rep.*, **5**, 958–963.
3. Bauer, P.O. and Nukina, N. (2009) The pathogenic mechanisms of polyglutamine diseases and current therapeutic strategies. *J. Neurochem.*, **110**, 1737–1765.
4. Luthi-Carter, R., Hanson, S.A., Strand, A.D., Bergstrom, D.A., Chun, W., Peters, N.L., Woods, A.M., Chan, E.Y., Kooperberg, C., Krainc, D. *et al.* (2002) Dysregulation of gene expression in the R6/2 model of polyglutamine disease: parallel changes in muscle and brain. *Hum. Mol. Genet.*, **11**, 1911–1926.
5. Chan, E.Y., Luthi-Carter, R., Strand, A., Solano, S.M., Hanson, S.A., DeJohn, M.M., Kooperberg, C., Chase, K.O., DiFiglia, M., Young, A.B. *et al.* (2002) Increased huntingtin protein length reduces the number of polyglutamine-induced gene expression changes in mouse models of Huntington's disease. *Hum. Mol. Genet.*, **11**, 1939–1951.
6. Kotliarova, S., Jana, N.R., Sakamoto, N., Kurosawa, M., Miyazaki, H., Nekooki, M., Doi, H., Machida, Y., Wong, H.K., Suzuki, T. *et al.* (2005) Decreased expression of hypothalamic neuropeptides in Huntington disease transgenic mice with expanded polyglutamine-EGFP fluorescent aggregates. *J. Neurochem.*, **93**, 641–653.
7. Kuhn, A., Goldstein, D.R., Hodges, A., Strand, A.D., Sengstag, T., Kooperberg, C., Becanovic, K., Pouladi, M.A., Sathasivam, K., Cha, J.H. *et al.* (2007) Mutant huntingtin's effects on striatal gene expression in mice recapitulate changes observed in human Huntington's disease brain and do not differ with mutant huntingtin length or wild-type huntingtin dosage. *Hum. Mol. Genet.*, **16**, 1845–1861.
8. Nucifora, F.C. Jr, Sasaki, M., Peters, M.F., Huang, H., Cooper, J.K., Yamada, M., Takahashi, H., Tsuji, S., Troncoso, J., Dawson, V.L. *et al.* (2001) Interference by huntingtin and atrophin-1 with cbp-mediated transcription leading to cellular toxicity. *Science*, **291**, 2423–2428.
9. Steffan, J.S., Kazantsev, A., Spasic-Boskovic, O., Greenwald, M., Zhu, Y.Z., Gohler, H., Wanker, E.E., Bates, G.P., Housman, D.E. and Thompson, L.M. (2000) The Huntington's disease protein interacts with p53 and CREB-binding protein and represses transcription. *Proc. Natl Acad. Sci. USA*, **97**, 6763–6768.
10. Suhr, S.T., Senut, M.C., Whitelegge, J.P., Faull, K.F., Cuizon, D.B. and Gage, F.H. (2001) Identities of sequestered proteins in aggregates from cells with induced polyglutamine expression. *J. Cell. Biol.*, **153**, 283–294.
11. van Roon-Mom, W.M., Reid, S.J., Jones, A.L., MacDonald, M.E., Faull, R.L. and Snell, R.G. (2002) Insoluble TATA-binding protein accumulation in Huntington's disease cortex. *Brain. Res. Mol. Brain. Res.*, **109**, 1–10.
12. Schaffar, G., Breuer, P., Boteva, R., Behrends, C., Tzvetkov, N., Strippel, N., Sakahira, H., Siegers, K., Hayer-Hartl, M. and Hartl, F.U. (2004) Cellular toxicity of polyglutamine expansion proteins: mechanism of transcription factor deactivation. *Mol. Cell.*, **15**, 95–105.
13. Dunah, A.W., Jeong, H., Griffin, A., Kim, Y.M., Standaert, D.G., Hersch, S.M., Mouradian, M.M., Young, A.B., Tanese, N. and Krainc, D. (2002) Sp1 and TAFII130 transcriptional activity disrupted in early Huntington's disease. *Science*, **296**, 2238–2243.
14. Li, S.H., Cheng, A.L., Zhou, H., Lam, S., Rao, M., Li, H. and Li, X.J. (2002) Interaction of Huntington disease protein with transcriptional activator Sp1. *Mol. Cell. Biol.*, **22**, 1277–1287.
15. Yamanaka, T., Miyazaki, H., Oyama, F., Kurosawa, M., Washizu, C., Doi, H. and Nukina, N. (2008) Mutant Huntingtin reduces HSP70 expression through the sequestration of NF-Y transcription factor. *EMBO J.*, **27**, 827–839.
16. Cha, J.H. (2000) Transcriptional dysregulation in Huntington's disease. *Trends Neurosci.*, **23**, 387–392.
17. Sugars, K.L. and Rubinsztein, D.C. (2003) Transcriptional abnormalities in Huntington disease. *Trends. Genet.*, **19**, 233–238.
18. Andersen, B. and Rosenfeld, M.G. (2001) POU domain factors in the neuroendocrine system: lessons from developmental biology provide insights into human disease. *Endocr. Rev.*, **22**, 2–35.
19. Nakai, S., Kawano, H., Yudate, T., Nishi, M., Kuno, J., Nagata, A., Jishage, K., Hamada, H., Fujii, H., Kawamura, K. *et al.* (1995) The POU domain transcription factor Brn-2 is required for the determination of specific neuronal lineages in the hypothalamus of the mouse. *Genes. Dev.*, **9**, 3109–3121.
20. Furukawa, Y., Kaneko, K., Matsumoto, G., Kurosawa, M. and Nukina, N. (2009) Cross-seeding fibrillation of Q/N-rich proteins offers new pathomechanism of polyglutamine diseases. *J. Neurosci.*, **29**, 5153–5162.
21. Busch, A., Engemann, S., Lurz, R., Okazawa, H., Lehrach, H. and Wanker, E.E. (2003) Mutant huntingtin promotes the fibrillogenesis of wild-type huntingtin: a potential mechanism for loss of huntingtin function in Huntington's disease. *J. Biol. Chem.*, **278**, 41452–41461.
22. Okazawa, H., Rich, T., Chang, A., Lin, X., Waragai, M., Kajikawa, M., Enokido, Y., Komuro, A., Kato, S., Shibata, M. *et al.* (2002) Interaction between mutant ataxin-1 and PQBP-1 affects transcription and cell death. *Neuron*, **34**, 701–713.
23. Waragai, M., Lammers, C.H., Takeuchi, S., Imafuku, I., Udagawa, Y., Kanazawa, I., Kawabata, M., Mouradian, M.M. and Okazawa, H. (1999) PQBP-1, a novel polyglutamine tract-binding protein, inhibits

transcription activation by Brn-2 and affects cell survival. *Hum. Mol. Genet.*, **8**, 977–987.

24. Zhai, W., Jeong, H., Cui, L., Krainc, D. and Tjian, R. (2005) In vitro analysis of huntingtin-mediated transcriptional repression reveals multiple transcription factor targets. *Cell*, **123**, 1241–1253.
25. Schonemann, M.D., Ryan, A.K., McEvilly, R.J., O'Connell, S.M., Arias, C.A., Kalla, K.A., Li, P., Sawchenko, P.E. and Rosenfeld, M.G. (1995) Development and survival of the endocrine hypothalamus and posterior pituitary gland requires the neuronal POU domain factor Brn-2. *Genes Dev.*, **9**, 3122–3135.
26. Wood, N.I., Goodman, A.O., van der Burg, J.M., Gazeau, V., Brundin, P., Bjorkqvist, M., Petersen, A., Tabrizi, S.J., Barker, R.A. and Morton, A.J. (2008) Increased thirst and drinking in Huntington's disease and the R6/2 mouse. *Brain Res. Bull.*, **76**, 70–79.
27. van der Burg, J.M., Bacos, K., Wood, N.I., Lindqvist, A., Wierup, N., Woodman, B., Wamsteeker, J.I., Smith, R., Deierborg, T., Kuhar, M.J. *et al.* (2008) Increased metabolism in the R6/2 mouse model of Huntington's disease. *Neurobiol. Dis.*, **29**, 41–51.
28. Keith, B., Adelman, D.M. and Simon, M.C. (2001) Targeted mutation of the murine arylhydrocarbon receptor nuclear translocator 2 (Arnt2) gene reveals partial redundancy with Arnt. *Proc. Natl Acad. Sci. USA*, **98**, 6692–6697.
29. Hosoya, T., Oda, Y., Takahashi, S., Morita, M., Kawauchi, S., Ema, M., Yamamoto, M. and Fujii-Kuriyama, Y. (2001) Defective development of secretory neurones in the hypothalamus of Arnt2-knockout mice. *Genes Cells*, **6**, 361–374.
30. Michaud, J.L., DeRossi, C., May, N.R., Holdener, B.C. and Fan, C.M. (2000) ARNT2 acts as the dimerization partner of SIM1 for the development of the hypothalamus. *Mech. Dev.*, **90**, 253–261.
31. Michaud, J.L., Rosenquist, T., May, N.R. and Fan, C.M. (1998) Development of neuroendocrine lineages requires the bHLH-PAS transcription factor SIM1. *Genes. Dev.*, **12**, 3264–3275.
32. Li, S.H. and Li, X.J. (2004) Huntingtin-protein interactions and the pathogenesis of Huntington's disease. *Trends Genet.*, **20**, 146–154.
33. Harjes, P. and Wanker, E.E. (2003) The hunt for huntingtin function: interaction partners tell many different stories. *Trends Biochem. Sci.*, **28**, 425–433.
34. Yu, Z.X., Li, S.H., Nguyen, H.P. and Li, X.J. (2002) Huntingtin inclusions do not deplete polyglutamine-containing transcription factors in HD mice. *Hum. Mol. Genet.*, **11**, 905–914.
35. Obrietan, K. and Hoyt, K.R. (2004) CRE-mediated transcription is increased in Huntington's disease transgenic mice. *J. Neurosci.*, **24**, 791–796.
36. Qiu, Z., Norflus, F., Singh, B., Swindell, M.K., Buzescu, R., Bejarano, M., Chopra, R., Zucker, B., Benn, C.L., DiRocco, D.P. *et al.* (2006) Sp1 is up-regulated in cellular and transgenic models of Huntington disease, and its reduction is neuroprotective. *J. Biol. Chem.*, **281**, 16672–16680.
37. Bae, B.I., Xu, H., Igarashi, S., Fujimuro, M., Agrawal, N., Taya, Y., Hayward, S.D., Moran, T.H., Montell, C., Ross, C.A. *et al.* (2005) p53 mediates cellular dysfunction and behavioral abnormalities in Huntington's disease. *Neuron*, **47**, 29–41.
38. Holbert, S., Denghien, I., Kiechle, T., Rosenblatt, A., Wellington, C., Hayden, M.R., Margolis, R.L., Ross, C.A., Dausset, J., Ferrante, R.J. *et al.* (2001) The Gln-Ala repeat transcriptional activator CA150 interacts with huntingtin: neuropathologic and genetic evidence for a role in Huntington's disease pathogenesis. *Proc. Natl Acad. Sci. USA*, **98**, 1811–1816.

39. Sugitani, Y., Nakai, S., Minowa, O., Nishi, M., Jishage, K., Kawano, H., Mori, K., Ogawa, M. and Noda, T. (2002) Brn-1 and Brn-2 share crucial roles in the production and positioning of mouse neocortical neurons. *Genes Dev.*, **16**, 1760–1765.
40. McEvilly, R.J., de Diaz, M.O., Schonemann, M.D., Hooshmand, F. and Rosenfeld, M.G. (2002) Transcriptional regulation of cortical neuron migration by POU domain factors. *Science*, **295**, 1528–1532.
41. Tagawa, K., Marubuchi, S., Qi, M.L., Enokido, Y., Tamura, T., Inagaki, R., Murata, M., Kanazawa, I., Wanker, E.E. and Okazawa, H. (2007) The induction levels of heat shock protein 70 differentiate the vulnerabilities to mutant huntingtin among neuronal subtypes. *J. Neurosci.*, **27**, 868–880.
42. Bjorkqvist, M., Petersen, A., Bacos, K., Isaacs, J., Norlen, P., Gil, J., Popovic, N., Sundler, F., Bates, G.P., Tabrizi, S.J. *et al.* (2006) Progressive alterations in the hypothalamic-pituitary-adrenal axis in the R6/2 transgenic mouse model of Huntington's disease. *Hum. Mol. Genet.*, **15**, 1713–1721.
43. Saleh, N., Moutereau, S., Durr, A., Krystkowiak, P., Azulay, J.P., Tranchant, C., Broussolle, E., Morin, F., Bachoud-Levi, A.C. and Maison, P. (2009) Neuroendocrine disturbances in Huntington's disease. *PLoS One*, **4**, e4962.
44. Petersen, A. and Bjorkqvist, M. (2006) Hypothalamic-endocrine aspects in Huntington's disease. *Eur. J. Neurosci.*, **24**, 961–967.
45. Donaldson, Z.R. and Young, L.J. (2008) Oxytocin, vasopressin, and the neurogenetics of sociality. *Science*, **322**, 900–904.
46. Timmers, H.J., Swaab, D.F., van de Nes, J.A. and Kremer, H.P. (1996) Somatostatin 1–12 immunoreactivity is decreased in the hypothalamic lateral tuberal nucleus of Huntington's disease patients. *Brain Res.*, **728**, 141–148.
47. Petersen, A., Gil, J., Maat-Schieman, M.L., Bjorkqvist, M., Tanila, H., Araujo, I.M., Smith, R., Popovic, N., Wierup, N., Norlen, P. *et al.* (2005) Orexin loss in Huntington's disease. *Hum. Mol. Genet.*, **14**, 39–47.
48. Sato, T., Miura, M., Yamada, M., Yoshida, T., Wood, J.D., Yazawa, I., Masuda, M., Suzuki, T., Shin, R.M., Yau, H.J. *et al.* (2009) Severe neurological phenotypes of Q129 DRPLA transgenic mice serendipitously created by en masse expansion of CAG repeats in Q76 DRPLA mice. *Hum. Mol. Genet.*, **18**, 723–736.
49. The FANTOM Consortium, Carninci, P., Kasukawa, T., Katayama, S., Gough, J., Frith, M.C., Maeda, N., Oyama, R. *et al.* (2005) The transcriptional landscape of the mammalian genome. *Science*, **309**, 1559–1563.
50. Doi, H., Mitsui, K., Kurosawa, M., Machida, Y., Kuroiwa, Y. and Nukina, N. (2004) Identification of ubiquitin-interacting proteins in purified polyglutamine aggregates. *FEBS Lett.*, **571**, 171–176.
51. Yamanaka, T., Horikoshi, Y., Izumi, N., Suzuki, A., Mizuno, K. and Ohno, S. (2006) Lgl mediates apical domain disassembly by suppressing the PAR-3-aPKC-PAR-6 complex to orient apical membrane polarity. *J. Cell. Sci.*, **119**, 2107–2118.
52. Oyama, F., Miyazaki, H., Sakamoto, N., Becquet, C., Machida, Y., Kaneko, K., Uchikawa, C., Suzuki, T., Kurosawa, M., Ikeda, T. *et al.* (2006) Sodium channel beta4 subunit: down-regulation and possible involvement in neuritic degeneration in Huntington's disease transgenic mice. *J. Neurochem.*, **98**, 518–529.